Structural Engineering and Mechanics, *Vol. 66, No. 3 (2018) 353-368*
DOI: https://doi.org/10.12989/sem.2018.66.3.353

Free vibration of FGM plates with porosity by a shear deformation theory with four variables

Mahfoud Yousfi[1,3], Hassen Ait Atmane[1,2], Mustapha Meradjah*[4], Abdelouahed Tounsi[1, 5] and Riadh Bennai[2]

[1]Material and Hydrology Laboratory, University of Sidi Bel Abbes, Faculty of Technology, Civil Engineering Department, Algeria
[2]Department of Civil Engineering, Faculty of Civil Engineering and Architecture, University of Chlef, Algeria
[3]Department of Civil Engineering, Faculty of Technology, University of Medea, Algeria
[4]Department of Civil Engineering, Faculty of Technology, University of Sidi Bel Abbes, Algeria
[5]Department of Civil and Environmental Engineering, King Fahd University of Petroleum & Minerals, 31261 Dhahran, Eastern Province, Saudi Arabia

(Received January 25, 2018, Revised February 12, 2018, Accepted February 14, 2018)

Abstract. In this work, a high order hyperbolic shear deformation theory with four variables is presented to study the vibratory behavior of functionally graduated plates. The field of displacement of the theory used in this work is introduced indeterminate integral variables. In addition, the effect of porosity is studied. It is assumed that the material characteristics of the porous FGM plate, varies continuously in the direction of thickness as a function of the power law model in terms of volume fractions of constituents taken into account the homogeneous distribution of porosity. The equations of motion are obtained using the principle of virtual work. An analytical solution of the Navier type for free vibration analysis is obtained for a FGM plate for simply supported boundary conditions. A comparison of the results obtained with those of the literature is made to verify the accuracy and efficiency of the present theory. It can be concluded from his results that the current theory is not only accurate but also simple for the presentation of the response of free vibration and the effect of porosity on the latter.

Keywords: high orders hyperbolic shear deformation theory; functionally graded plate; porosity; free vibration

1. Introduction

Functionally graded materials or functionally graded materials is a new class of materials that has attracted special attention and interest over the last three decades thanks to the advantage of continuity of physical properties in one or more directions. Their use is growing in aeronautics and aerospace where they can serve as thermal barriers to their rich ceramic composition. However, FGMs cover a wide range of applications in many other fields such as mechanics, medicine, civil engineering, electricity, nuclear, etc. (Bouderba *et al*. 2013, Tounsi *et al*. 2013, Kar and Panda 2013, 2014, Ahmed 2014, Zidi *et al*. 2014, Kar and Panda 2015a, b, c, d, Zemri *et al*. 2015, Taibi *et al*. 2015, Kar *et al*. 2016, Boukhari *et al*. 2016, Bounouara *et al*. 2016, Kar and Panda 2016a, b, c, d, e, Aldousari 2017, Abdelaziz *et al*. 2017, Sekkal *et al*. 2017a, Kar *et al*. 2017, Kar and Panda 2017, Bellifa *et al*. 2017a, Benadouda *et al*. 2017, Mouffoki *et al*. 2017, Attia *et al*. 2018, Shahsavari *et al*. 2018, Zine *et al*. 2018, Kaci *et al*. 2018, Fourn *et al*. 2018). It was the Japanese, in 1984, who introduced for the first time this new philosophy of intelligent materials able to withstand very large temperature gradients (Koizumi 1997). Generally, FGMs are multi-layered materials made by different components such as ceramic and metal. The use of this type of material in the structures requires a good understanding of the mechanical behavior of the FGM structures in order to offer an optimum profile to the designers. For this, several studies concerning the study of the mechanical behavior of FGM plates are announced on the analysis of the dynamic behavior of FGM structures. For example, Reddy (2000) has analyzed the static behavior of FGM rectangular plates based on his third-order shear deformation plate theory. Reddy and Cheng (2001) have presented a three-dimensional model for an FGM plate subjected to mechanical and thermal loads, both applied at the top of the plate. Woo *et al*. (2006) studied the non-linear free vibration behavior of plates made of FGMs using the Von Karman theory for large transverse deflection. In addition, Park and Kim (2006) investigated the thermal post buckling and vibration analyses of FG plates. Sobhy (2013) studied the vibration and buckling behavior of exponentially graded material sandwich plate resting on elastic foundations under various boundary conditions. Chakraverty and Pradhan (2014) studied the free vibration of exponential functionally graded rectangular plates in thermal environment with general boundary conditions. Hebali *et al*. (2014) developed a new quasi-3D hyperbolic shear deformation theory for the bending and free vibration behavior of FG plate. Belabed *et al*. (2014) used a hyperbolic function based higher-order shear deformation theory to analysis the vibration characteristics of FGM plate. Vo *et al*. (2015) studied vibration and buckling responses of FG sandwich beams by using a quasi-3D

*Corresponding author, Ph.D.
E-mail: mdjh_mus@yahoo.fr

http://www.techno-press.com/journals/sem&subpage=7 ISSN: 1225-4568 (Print), 1598-6217 (Online)

theory. Bennai *et al*. (2015) proposed a novel higher-order shear and normal deformation theory for the study of vibration and stability for FG sandwich beams. Mahi *et al*. (2015) developed a novel hyperbolic shear deformation model for static and dynamic analysis of isotropic, functionally graded, sandwich and laminated composite plates. Belkorissat *et al*. (2015) studied the dynamic properties of FG nanoscale plates using a novel nonlocal refined four variable theory. Mehar *et al*. (2016) presented vibration analysis of functionally graded carbon nanotube reinforced composite plate in thermal environment. Bouderba *et al*. (2016) studied the thermal stability of FG sandwich plates using a simple shear deformation theory. Bousahla *et al*. (2016) analyzed the thermal buckling behaviour of plates with FG coefficient of thermal expansion. Bellifa *et al*. (2016) presented static bending and dynamic analysis of FG plates using a simple shear deformation theory and the concept the neutral surface position. Beldjelili *et al*. (2016) analyzed the hygro-thermo-mechanical bending response of S-FGM plates resting on variable elastic foundations using a four-variable trigonometric plate theory. Houari *et al*. (2016) presented a new simple three-unknown sinusoidal shear deformation theory for FG plates. Draiche *et al*. (2016) used a refined theory with stretching effect for the flexure analysis of laminated composite plates. Bennoun *et al*. (2016) studied the vibration response of FG sandwich plates using a novel five variable refined plate theory. Bellifa *et al*. (2017b) proposed a nonlocal zeroth-order shear deformation theory for nonlinear postbuckling of nanobeams. Kolahchi *et al*. (2017) discussed wave propagation problem of embedded viscoelastic FG-CNT-reinforced sandwich plates integrated with sensor and actuator based on refined zigzag theory. Chikh *et al*. (2017) investigated the thermal buckling of cross-ply laminated plates using a simplified HSDT. Mehar and Panda (2017) presented an experimental, numerical, and simulation study for elastic bending and stress analysis of carbon nanotube-reinforced composite plate. Mehar *et al*. (2017a) presented also a theoretical and experimental investigation of vibration characteristic of carbon nanotube reinforced polymer composite structure. Mehar *et al*. (2017b) provided nonlinear thermoelastic frequency analysis of functionally graded CNT-reinforced single/doubly curved shallow shell panels by FEM.

During the production of FGM materials, pores may occur within its materials during the sintering step because of the large difference in solidification temperatures between the components of the material (Zhu *et al*. 2001). Wattanasakulpong *et al*. (2012) gives the discussion on porosities happening inside FGM samples fabricated by a multi-step sequential infiltration technique. Wattanasakulpong and Ungbhakorn (2014) also investigate linear and nonlinear vibration problems of FGM beams having porosities. Ait Atmane *et al*. (2015) presented a computational shear displacement model for vibrational analysis of FG beams with porosities. Ait Yahia *et al*. (2015) investigated the wave propagation in FG plates with considering the porosity effect. Recently, Jahwari and Naguib (2016) investigated FG viscoelastic porous plates with a higher order plate theory and a statistical based model of cellular distribution. Mouaici *et al*. (2016) proposed an analytical solution for the vibration of FGM plates with porosities. The analysis was based on the deformation theory of shear with taking into account the exact position of the neutral surface. Ait Atmane *et al*. (2017) is study the effect of stretching the thickness and porosity on the mechanical response of a FG beam resting on elastic foundations. Akbas (2017) studied the thermal effects on the vibratory behaviour of FG beams with porosity.

In this work, an analytical study of the free vibration of FGM porous plates simply supported using a new displacement model was presented. The plates are made of an isotropic material with material properties varying in the direction of thickness. Equations of the FG plate is obtained using the Hamilton principle. To solve the problem, the Navier solution is also used. At the end, numerical results for the effect of porosity and material distribution parameters on natural frequencies of FGM plates are presented. The effectiveness of the present theory is verified by comparing the results obtained with those found in the literature.

2. Properties of the FGM constituent materials

A FG plate made from a mixture of two material phases, for example, a metal and a ceramic. The material properties of FG plate are assumed to vary continuously through the thickness of the plate. In this investigation, the imperfect plate is assumed to have porosities spreading within the thickness due to defect during production. Consider an imperfect FGM with a porosity volume fraction, a(a<< 1), distributed evenly among the metal and ceramic, the modified rule of mixture proposed by Wattanasakulpong and Ungbhakorn (2014) is used as

$$P(z) = P_m\left(V_m - \frac{\alpha}{2}\right) + P_c\left(V_c - \frac{\alpha}{2}\right) \tag{1}$$

Now, the total volume fraction of the metal and ceramic is Vm + Vc = 1, and the power law of volume fraction of the ceramic is described as

$$V_C = \left(\frac{z}{h} + \frac{1}{2}\right)^k \tag{2}$$

Hence, all properties of the imperfect FGM can be written as

$$P(z) = P_m + (P_c - P_m)\left(\frac{1}{2} + \frac{z}{h}\right)^p - (P_c + P_m)\frac{\alpha}{2} \tag{3}$$

It is noted that the positive real number p($0 \le p < \infty$) is the power law or volume fraction index, and z is the distance from the mid-plane of the FG plate. The FG plate becomes a fully ceramic plate when k is set to zero and fully metal for large value of ρ. Thus, the Young's modulus (E) and material density (ρ) equations of the imperfect FGM plate can be expressed as

$$E(z) = E_m + (E_c - E_m)\left(\frac{1}{2} + \frac{z}{h}\right)^p - (E_c + E_m)\frac{\alpha}{2} \tag{4}$$

$$\rho(z)=\rho_m+(\rho_c-\rho_m)\left(\frac{1}{2}+\frac{z}{h}\right)^p-(\rho_c+\rho_m)\frac{\alpha}{2} \tag{5}$$

Since the influences of the variation of Poisson's ratio (v) on the behaviour of FG plates are very small (Yang *et al.* 2005, Kitipornchai *et al.* 2006), it is supposed to be constant for convenience.

In addition, for another scenario of porosity distribution, it is possible to obtain imperfect FGM samples, which have almost porosities spreading around the middle zone of the cross-section, and the amount of porosity seems to be on the decrease to zero at the top and bottom of the cross-section. Based on the principle of the multi-step sequential infiltration technique that can be employed to fabricate FGM samples (Wattanasakulpong *et al.* 2012), the porosities mostly occur at the middle zone. At this zone, it is difficult to infiltrate the materials completely, while at the top and bottom zones, the process of material infiltration can be performed easier and leaves less porosity. Consider this scenario, the equations of Young's modulus (E) and material density (ρ) in Eqs. (4)-(5) are replaced by the following forms

$$E(z)=E_m+(E_c-E_m)\left(\frac{1}{2}+\frac{z}{h}\right)^p-(E_c+E_m)\frac{\alpha}{2}\left(1-\frac{2|z|}{h}\right) \tag{6}$$

$$\rho(z)=\rho_m+(\rho_c-\rho_m)\left(\frac{1}{2}+\frac{z}{h}\right)^p-(\rho_c+\rho_m)\frac{\alpha}{2}\left(1-\frac{2|z|}{h}\right) \tag{7}$$

3. Fundamental equations

3.1 Kinematics and strains

In this work, other simplifying hypotheses are made to the presented theory in order to minimize the number of unknowns. The displacement field of the conventional theory is given by (Bakhadda *et al.* 2018, Belabed *et al.* 2018)

$$u(x,y,z,t)=u_0(x,y,t)-z\frac{\partial w_0}{\partial x}+f(z)\varphi_x(x,y,t) \tag{8a}$$

$$v(x,y,z,t)=v_0(x,y,t)-z\frac{\partial w_0}{\partial y}+f(z)\varphi_y(x,y,t) \tag{8b}$$

$$w(x,y,z,t)=w_0(x,y,t) \tag{8c}$$

where u_0; v_0; w_0, φ_x, φ_y are five unknown displacements of the mid-plane of the plate, $f(z)$ denotes shape function representing the variation of the transverse shear strains and stresses within the thickness. By considering that (Menasria et al. 2017, Besseghier *et al.* 2017, El-Haina *et al.* 2017, Fahsi *et al.* 2017, Khetir *et al.* 2017, Yazid *et al.* 2018) $\varphi_x=\int\theta(x,y)dx$ and $\varphi_y=\int\theta(x,y)dy$, the displacement field of the present model can be expressed in a simpler form as

$$u(x,y,z,t)=u_0(x,y,t)-z\frac{\partial w_0}{\partial x}+k_1\,f(z)\int\theta(x,y,t)\,dx \tag{9a}$$

$$v(x,y,z,t)=v_0(x,y,t)-z\frac{\partial w_0}{\partial y}+k_2\,f(z)\int\theta(x,y,t)\,dy \tag{9b}$$

$$w(x,y,z,t)=w_0(x,y,t) \tag{9c}$$

In this work, the present higher-order shear deformation plate theory is obtained by setting

$$f(z)=z\left(\frac{5}{4}-\frac{5z^2}{3h^2}\right) \tag{10}$$

It can be seen that the displacement field in Eq. (9) introduces only four unknowns (u_0, v_0, w_0 and θ). The nonzero strains associated with the displacement field in Eq. (9) are

$$\begin{Bmatrix}\varepsilon_x\\ \varepsilon_y\\ \gamma_{xy}\end{Bmatrix}=\begin{Bmatrix}\varepsilon_x^0\\ \varepsilon_y^0\\ \gamma_{xy}^0\end{Bmatrix}+z\begin{Bmatrix}k_x^b\\ k_y^b\\ k_{xy}^b\end{Bmatrix}+f(z)\begin{Bmatrix}k_x^s\\ k_y^s\\ k_{xy}^s\end{Bmatrix}$$
$$\begin{Bmatrix}\gamma_{yz}\\ \gamma_{xz}\end{Bmatrix}=g(z)\begin{Bmatrix}\gamma_{yz}^0\\ \gamma_{xz}^0\end{Bmatrix} \tag{11}$$

Where

$$\begin{Bmatrix}\varepsilon_x^0\\ \varepsilon_y^0\\ \gamma_{xy}^0\end{Bmatrix}=\begin{Bmatrix}\dfrac{\partial u_0}{\partial x}\\ \dfrac{\partial v_0}{\partial x}\\ \dfrac{\partial u_0}{\partial y}+\dfrac{\partial v_0}{\partial x}\end{Bmatrix},\ \begin{Bmatrix}k_x^b\\ k_y^b\\ k_{xy}^b\end{Bmatrix}=\begin{Bmatrix}-\dfrac{\partial^2 w_0}{\partial x^2}\\ -\dfrac{\partial^2 w_0}{\partial y^2}\\ -2\dfrac{\partial^2 w_0}{\partial x\partial y}\end{Bmatrix},$$
$$\begin{Bmatrix}k_x^s\\ k_y^s\\ k_{xy}^s\end{Bmatrix}=\begin{Bmatrix}k_1\theta\\ k_2\theta\\ k_1\dfrac{\partial}{\partial y}\displaystyle\int\theta\,dx+k_2\dfrac{\partial}{\partial x}\int\theta\,dy\end{Bmatrix}, \tag{12a}$$
$$\begin{Bmatrix}\gamma_{yz}^0\\ \gamma_{xz}^0\end{Bmatrix}=\begin{Bmatrix}k_2\displaystyle\int\theta\,dy\\ k_1\displaystyle\int\theta\,dx\end{Bmatrix}$$

and

$$g(z)=\frac{df(z)}{dz} \tag{12b}$$

The integrals defined in the above equations shall be resolved by a Navier type method and can be written as follows

$$\frac{\partial}{\partial y}\int\theta\,dx=A'\frac{\partial^2\theta}{\partial x\partial y},\ \frac{\partial}{\partial x}\int\theta\,dy=B'\frac{\partial^2\theta}{\partial x\partial y}, \tag{13}$$

$$\int \theta\, dx = A' \frac{\partial \theta}{\partial x}, \quad \int \theta\, dy = B' \frac{\partial \theta}{\partial y}$$

where the coefficients A' and B' are expressed according to the type of solution used, in this case via Navier. Therefore, A', B', k_1 and k_2 are expressed as follows

$$A' = -\frac{1}{\alpha^2}, \; B' = -\frac{1}{\beta^2}, \; k_1 = \alpha^2, \; k_2 = \beta^2 \tag{14}$$

where α and β are defined in expression (30).

For elastic and isotropic FGMs, the constitutive relations can be expressed as

$$\begin{Bmatrix} \sigma_x \\ \sigma_y \\ \tau_{xy} \\ \tau_{yz} \\ \tau_{xz} \end{Bmatrix} = \begin{bmatrix} C_{11} & C_{12} & 0 & 0 & 0 \\ C_{12} & C_{22} & 0 & 0 & 0 \\ 0 & 0 & C_{66} & 0 & 0 \\ 0 & 0 & 0 & C_{44} & 0 \\ 0 & 0 & 0 & 0 & C_{55} \end{bmatrix} \begin{Bmatrix} \varepsilon_x \\ \varepsilon_y \\ \gamma_{xy} \\ \gamma_{yz} \\ \gamma_{xz} \end{Bmatrix} \tag{15}$$

where (σ_x, σ_y, τ_{xy}, τ_{yz}, τ_{xz}) and (ε_x, ε_y, γ_{xy}, γ_{yz}, γ_{xz}) are the stress and strain components, respectively. Using the material properties defined in Eq. (1), stiffness coefficients, C_{ij}, can be given as

$$\begin{aligned} C_{11} = C_{22} &= \frac{E(z)}{1-\nu^2}, \; C_{12} = \frac{\nu\, E(z)}{1-\nu^2}, \\ C_{44} = C_{55} = C_{66} &= \frac{E(z)}{2(1+\nu)}, \end{aligned} \tag{16}$$

3.2 Equations of motion

To determine the equations of motion, we apply the principle of Hamilton (Meksi *et al.* 2018, Youcef *et al.* 2018, Hachemi *et al.* 2017, Zidi *et al.* 2017, Klouche *et al.* 2017, Ahouel *et al.* 2016, Al-Basyouni *et al.* 2015, Attia *et al.* 2015, Ait Amar Meziane *et al.* 2014)

$$0 = \int_0^t (\delta U + \delta V - \delta K)\, dt \tag{17}$$

where δU is the variation of strain energy; δV is the variation of the external work done by external load applied to the plate; and δK is the variation of kinetic energy.

The variation of strain energy of the plate is given by

$$\begin{aligned} \delta U &= \int_V \left[\sigma_x \delta\varepsilon_x + \sigma_y \delta\varepsilon_y + \tau_{xy}\delta\gamma_{xy} + \tau_{yz}\delta\gamma_{yz} + \tau_{xz}\delta\gamma_{xz}\right] dV \\ &= \int_A \Big[N_x \delta\varepsilon_x^0 + N_y \delta\varepsilon_y^0 + N_{xy}\delta\gamma_{xy}^0 + M_x^b \delta k_x^b + M_y^b \delta k_y^b + M_{xy}^b \delta k_{xy}^b \\ &\quad + M_x^s \delta k_x^s + M_y^s \delta k_y^s + M_{xy}^s \delta k_{xy}^s + S_{yz}^s \delta\gamma_{yz}^s + S_{xz}^s \delta\gamma_{xz}^0\Big] dA = 0 \end{aligned} \tag{18}$$

where A is the top surface and the stress resultants N, M, and S are defined by

$$\left(N_i, M_i^b, M_i^s\right) = \int_{-h/2}^{h/2} (1, z, f)\sigma_i\, dz, \quad (i = x, y, xy), \tag{19}$$

$$\left(S_{xz}^s, S_{yz}^s\right) = \int_{-h/2}^{h/2} g\left(\tau_{xz}, \tau_{yz}\right) dz$$

The variation of the external work can be expressed as

$$\delta V = -\int_A q\delta w_0\, dA - \int_A \begin{pmatrix} N_x^0 \dfrac{\partial w_0}{\partial x}\dfrac{\partial \delta w_0}{\partial x} + 2N_{xy}^0 \dfrac{\partial w_0}{\partial x}\dfrac{\partial \delta w_0}{\partial y} + \\ N_y^0 \dfrac{\partial w_0}{\partial y}\dfrac{\partial \delta w_0}{\partial y} \end{pmatrix} dA \tag{20}$$

where q and (N_x^0, N_y^0, N_{xy}^0)are transverse and in-plane applied loads, respectively.

The variation of kinetic energy of the plate can be expressed as

$$\begin{aligned} \delta K &= \int_V \left[\dot{u}\delta\dot{u} + \dot{v}\delta\dot{v} + \dot{w}\delta\dot{w}\right] \rho(z)\, dV \\ &= \int_A \Big\{ I_0\left[\dot{u}_0\delta\dot{u}_0 + \dot{v}_0\delta\dot{v}_0 + \dot{w}_0\delta\dot{w}_0\right] \\ &- I_1\left(\dot{u}_0\frac{\partial\delta\dot{w}_0}{\partial x} + \frac{\partial\dot{w}_0}{\partial x}\delta\dot{u}_0 + \dot{v}_0\frac{\partial\delta\dot{w}_0}{\partial y} + \frac{\partial\dot{w}_0}{\partial y}\delta\dot{v}_0\right) \\ &+ J_1\left((k_1 A')\left(\dot{u}_0\frac{\partial\delta\dot{\theta}}{\partial x} + \frac{\partial\dot{\theta}}{\partial x}\delta\dot{u}_0\right) + (k_2 B')\left(\dot{v}_0\frac{\partial\delta\dot{\theta}}{\partial y} + \frac{\partial\dot{\theta}}{\partial y}\delta\dot{v}_0\right)\right) \\ &+ I_2\left(\frac{\partial\dot{w}_0}{\partial x}\frac{\partial\delta\dot{w}_0}{\partial x} + \frac{\partial\dot{w}_0}{\partial y}\frac{\partial\delta\dot{w}_0}{\partial y}\right) + K_2\left((k_1 A')^2\left(\frac{\partial\dot{\theta}}{\partial x}\frac{\partial\delta\dot{\theta}}{\partial x}\right) + (k_2 B')^2\left(\frac{\partial\dot{\theta}}{\partial y}\frac{\partial\delta\dot{\theta}}{\partial y}\right)\right) \\ &- J_2\left((k_1 A')\left(\frac{\partial\dot{w}_0}{\partial x}\frac{\partial\delta\dot{\theta}}{\partial x} + \frac{\partial\dot{\theta}}{\partial x}\frac{\partial\delta\dot{w}_0}{\partial x}\right) + (k_2 B')\left(\frac{\partial\dot{w}_0}{\partial y}\frac{\partial\delta\dot{\theta}}{\partial y} + \frac{\partial\dot{\theta}}{\partial y}\frac{\partial\delta\dot{w}_0}{\partial y}\right)\right)\Big\} dA \end{aligned} \tag{21}$$

the differentiation with respect to the time variable t; $\rho(z)$ is the mass density given by Eq. (7); and (I_i, J_i, K_i) are mass inertias expressed by

$$\left(I_0, I_1, I_2\right) = \int_{-h/2}^{h/2} \left(1, z, z^2\right)\rho(z)\, dz \tag{22a}$$

$$\left(J_1, J_2, K_2\right) = \int_{-h/2}^{h/2} \left(f, z\, f, f^2\right)\rho(z)\, dz \tag{22b}$$

By substituting Eqs. (18), (20) and (21) into Eq. (17), the following can be derived

$$\begin{aligned} &\delta u_0: \; \frac{\partial N_x}{\partial x} + \frac{\partial N_{xy}}{\partial y} = I_0\ddot{u}_0 - I_1\frac{\partial\ddot{w}_0}{\partial x} + k_1 A' J_1\frac{\partial\ddot{\theta}}{\partial x} \\ &\delta v_0: \; \frac{\partial N_{xy}}{\partial x} + \frac{\partial N_y}{\partial y} = I_0\ddot{v}_0 - I_1\frac{\partial\ddot{w}_0}{\partial y} + k_2 B' J_1\frac{\partial\ddot{\theta}}{\partial y} \\ &\delta w_0: \; \frac{\partial^2 M_x^b}{\partial x^2} + 2\frac{\partial^2 M_{xy}^b}{\partial x\partial y} + \frac{\partial^2 M_y^b}{\partial y^2} = I_0\ddot{w}_0 + I_1\left(\frac{\partial\ddot{u}_0}{\partial x} + \frac{\partial\ddot{v}_0}{\partial y}\right) - \\ &I_2\nabla^2\ddot{w}_0 + J_2\left(k_1 A'\frac{\partial^2\ddot{\theta}}{\partial x^2} + k_2 B'\frac{\partial^2\ddot{\theta}}{\partial y^2}\right) \\ &\delta\theta: \; -k_1 M_x^s - k_2 M_y^s - (k_1 A' + k_2 B')\frac{\partial^2 M_{xy}^s}{\partial x\partial y} + k_1 A'\frac{\partial S_{xz}^s}{\partial x} + k_2 B'\frac{\partial S_{yz}^s}{\partial y} = \\ &-J_1\left(k_1 A'\frac{\partial\ddot{u}_0}{\partial x} + k_2 B'\frac{\partial\ddot{v}_0}{\partial y}\right) - K_2\left((k_1 A')^2\frac{\partial^2\ddot{\theta}}{\partial x^2} + (k_2 B')^2\frac{\partial^2\ddot{\theta}}{\partial y^2}\right) + \\ &J_2\left(k_1 A'\frac{\partial^2\ddot{w}_0}{\partial x^2} + k_2 B'\frac{\partial^2\ddot{w}_0}{\partial y^2}\right) \end{aligned} \tag{23}$$

Substituting Eq. (11) into Eq. (15) and the subsequent results into Eqs. (19), the stress resultants are obtained in terms of strains as following compact form

$$\begin{Bmatrix} N \\ M^b \\ M^s \end{Bmatrix} = \begin{bmatrix} A & B & B^s \\ B & D & D^s \\ B^s & D^s & H^s \end{bmatrix} \begin{Bmatrix} \varepsilon \\ k^b \\ k^s \end{Bmatrix}, S = A^s \gamma \tag{24}$$

in which

$$N = \{N_x, N_y, N_{xy}\}^t, \quad M^b = \{M_x^b, M_y^b, M_{xy}^b\}^t, \quad M^s = \{M_x^s, M_y^s, M_{xy}^s\}^t \tag{25a}$$

$$\varepsilon = \{\varepsilon_x^0, \varepsilon_y^0, \gamma_{xy}^0\}^t, \quad k^b = \{k_x^b, k_y^b, k_{xy}^b\}^t, \quad k^s = \{k_x^s, k_y^s, k_{xy}^s\}^t \tag{25b}$$

$$A = \begin{bmatrix} A_{11} & A_{12} & 0 \\ A_{12} & A_{22} & 0 \\ 0 & 0 & A_{66} \end{bmatrix}, \quad B = \begin{bmatrix} B_{11} & B_{12} & 0 \\ B_{12} & B_{22} & 0 \\ 0 & 0 & B_{66} \end{bmatrix}, \quad D = \begin{bmatrix} D_{11} & D_{12} & 0 \\ D_{12} & D_{22} & 0 \\ 0 & 0 & D_{66} \end{bmatrix} \tag{25c}$$

$$B^s = \begin{bmatrix} B_{11}^s & B_{12}^s & 0 \\ B_{12}^s & B_{22}^s & 0 \\ 0 & 0 & B_{66}^s \end{bmatrix}, \quad D^s = \begin{bmatrix} D_{11}^s & D_{12}^s & 0 \\ D_{12}^s & D_{22}^s & 0 \\ 0 & 0 & D_{66}^s \end{bmatrix}, \quad H^s = \begin{bmatrix} H_{11}^s & H_{12}^s & 0 \\ H_{12}^s & H_{22}^s & 0 \\ 0 & 0 & H_{66}^s \end{bmatrix} \tag{25d}$$

$$S = \{S_{xz}^s, S_{yz}^s\}^t, \gamma = \{\gamma_{xz}^0, \gamma_{yz}^0\}^t, A^s = \begin{bmatrix} A_{44}^s & 0 \\ 0 & A_{55}^s \end{bmatrix} \tag{25e}$$

and stiffness components are given as

$$\begin{Bmatrix} A_{11} & B_{11} & D_{11} & B_{11}^s & D_{11}^s & H_{11}^s \\ A_{12} & B_{12} & D_{12} & B_{12}^s & D_{12}^s & H_{12}^s \\ A_{66} & B_{66} & D_{66} & B_{66}^s & D_{66}^s & H_{66}^s \end{Bmatrix} = \int_{-h/2}^{h/2} C_{11}\left(1, z, z^2, f(z), z\, f(z), f^2(z)\right) \begin{Bmatrix} 1 \\ \nu \\ \dfrac{1-\nu}{2} \end{Bmatrix} dz \tag{26a}$$

$$\left(A_{22}, B_{22}, D_{22}, B_{22}^s, D_{22}^s, H_{22}^s\right) = \left(A_{11}, B_{11}, D_{11}, B_{11}^s, D_{11}^s, H_{11}^s\right) \tag{26b}$$

$$A_{44}^s = A_{55}^s = \int_{-h/2}^{h/2} C_{44}[g(z)]^2 dz, \tag{26c}$$

Introducing Eq. (24) into Eq. (23), the equations of motion can be expressed in terms of displacements (u_0, v_0, w_0, θ) and the appropriate equations take the form

$$\begin{aligned} &A_{11}d_{11}u_0 + A_{66}\, d_{22}u_0 + (A_{12} + A_{66})d_{12}v_0 - B_{11}d_{111}w_0 - \\ &(B_{12} + 2B_{66})d_{122}w_0 + \left(B_{66}^s(k_1 A' + k_2\, B')\right) d_{122}\theta + \\ &\left(B_{11}^s k_1 + B_{12}^s\, k_2\right) d_1\theta = I_0\ddot{u}_0 - I_1\, d_1\ddot{w}_0 + J_1\, A' k_1 d_1\ddot{\theta}, \end{aligned} \tag{27a}$$

$$\begin{aligned} &A_{22}\, d_{22}v_0 + A_{66}\, d_{11}v_0 + (A_{12} + A_{66})\, d_{12}u_0 - B_{22}\, d_{222}w_0 - \\ &(B_{12} + 2B_{66})\, d_{112}w_0 + \left(B_{66}^s\, (k_1 A' + k_2\, B')\right) d_{112}\theta + \\ &\left(B_{22}^s k_2 + B_{12}^s k_1\right) d_2\theta = I_0\ddot{v}_0 - I_1\, d_2\ddot{w}_0 + J_1\, B' k_2\, d_2\ddot{\theta}, \end{aligned} \tag{27b}$$

$$\begin{aligned} &B_{11}\, d_{111}u_0 + (B_{12} + 2B_{66})d_{122}u_0 + (B_{12} + 2B_{66})d_{112}v_0 + \\ &B_{22}\, d_{222}v_0 - D_{11}d_{1111}w_0 - 2(D_{12} + 2D_{66})\, d_{1122}w_0 - \\ &D_{22}\, d_{2222}w_0 + \left(D_{11}^s\, k_1 + D_{12}^s\, k_2\right) d_{11}\theta + 2\left(D_{66}^s\,(k_1 A' + k_2 B')\right) d_{1122}\theta + \\ &\left(D_{12}^s k_1 + D_{22}^s k_2\right) d_{22}\theta = I_0\ddot{w}_0 + I_1\left(d_1\ddot{u}_0 + d_2\,\ddot{v}_0\right) - I_2\left(d_{11}\ddot{w}_0 + d_{22}\ddot{w}_0\right) \\ &+ J_2\left(k_1 A'\, d_{11}\ddot{\theta} + k_2\, B'\, d_{22}\ddot{\theta}\right) \end{aligned} \tag{27c}$$

$$\begin{aligned} &-\left(B_{11}^s k_1 + B_{12}^s k_2\right)d_1 u_0 - \left(B_{66}^s\,(k_1 A' + k_2 B')\right)d_{122}u_0 - \\ &\left(B_{66}^s\,(k_1 A' + k_2 B')\right) d_{112}v_0 - \left(B_{12}^s k_1 + B_{22}^s k_2\right)d_2 v_0 \\ &+ \left(D_{11}^s k_1 + D_{12}^s k_2\right)d_{11}w_0 + 2\,\left(D_{66}^s\,(k_1 A' + k_2 B')\right)d_{1122}w_0 + \\ &\left(D_{12}^s k_1 + D_{22}^s k_2\right)d_{22}w_0 - H_{11}^s\, k_1^2\,\theta - H_{22}^s\, k_2^2\,\theta - 2H_{12}^s\, k_1\, k_2\theta \\ &- \left((k_1 A' + k_2 B')^2 H_{66}^s\right)d_{1122}\theta + A_{44}^s\,(k_2 B')^2\, d_{22}\theta + A_{55}^s\,(k_1\, A')^2\, d_{11}\theta = \\ &-J_1\left(k_1\, A' d_1\ddot{u}_0 + k_2\, B' d_2\ddot{v}_0\right) + J_2\left(k_1\, A' d_{11}\ddot{w}_0 + k_2\, B' d_{22}\ddot{w}_0\right) - \\ &K_2\left((k_1 A')^2\, d_{11}\ddot{\theta} + (k_2\, B')^2 d_{22}\ddot{\theta}\right) \end{aligned} \tag{27c}$$

where d_{ij}, d_{ijl} and d_{ijlm} are the following differential operators

$$d_{ij} = \frac{\partial^2}{\partial x_i \partial x_j}, d_{ijl} = \frac{\partial^3}{\partial x_i \partial x_j \partial x_l}, \quad d_{ijlm} = \frac{\partial^4}{\partial x_i \partial x_j \partial x_l \partial x_m}, d_i = \frac{\partial}{\partial x_i}, (i, j, l, m = 1,2). \tag{28}$$

3.3 Analytical solution for simply-supported FG plates

The Navier solution method is employed to determine the analytical solutions for which the displacement variables are written as product of arbitrary parameters and known trigonometric functions to respect the equations of motion and boundary conditions.

$$\begin{Bmatrix} u_0 \\ v_0 \\ w_0 \\ \theta \end{Bmatrix} = \sum_{m=1}^{\infty}\sum_{n=1}^{\infty} \begin{Bmatrix} U_{mn} e^{i\omega t} \cos(\alpha\, x)\sin(\beta\, y) \\ V_{mn} e^{i\omega t} \sin(\alpha\, x)\cos(\beta\, y) \\ W_{mn} e^{i\omega t} \sin(\alpha\, x)\sin(\beta\, y) \\ X_{mn} e^{i\omega t} \sin(\alpha\, x)\sin(\beta\, y) \end{Bmatrix} \tag{29}$$

where ω is the frequency of free vibration of the plate, $\sqrt{i} = -1$ the imaginary unit.

with

$$\alpha = m\pi / a\,, \quad \beta = n\pi / b \tag{30}$$

The transverse load q is also expanded in the double-Fourier sine series as

$$q(x, y) = \sum_{m=1}^{\infty}\sum_{n=1}^{\infty} Q_{mn} \sin(\alpha\, x)\sin(\beta\, y) \tag{31}$$

where

Table 1 Comparison of fundamental frequency parameter $\bar{\beta}$ of Al/ZrO_2 square plate

		p=1			a/h=5		
Theory	Porosity	a/h=5	a/h=10	a/h=20	P=2	P=3	P=5
Vel and Batra (2004) 3-D		0.2192	0.0596	0.0153	0.2197	0.2211	0.2225
Matsunaga (2008) HSDT		0.2285	0.0619	0.0158	0.2264	0.2270	0.2281
Hosseini- Hashemi *et al*. (2011b) HSDT	α=0	0.2276	0.0619	0.0158	0.2256	0.2263	0.2272
Hosseini- Hashemi *et al*. (2011c) FSDT		0.2276	0.0619	0.0158	0.2264	0.2276	0.2291
CPT		0.2479	0.0634	0.0159	0.2473	0.2497	0.2526
	α=0	0.2276	0.0618	0.0158	0.2257	0.2263	0.2272
Mouaici *et al*. (2016)	α=0.1	0.2258	0.0612	0.0156	0.2228	0.2233	0.2244
	α=0.2	0.2231	0.0604	0.0154	0.2184	0.2186	0.2199
	α=0	0,2276	0,0618	0,0158	0,2256	0,2262	0,2271
Present	α=0.1	0,2258	0,0612	0,0156	0,2228	0,2232	0,2243
	α=0.2	0,2231	0,0604	0,0154	0,2184	0,2185	0,2197

$$Q_{mn} = \frac{4}{ab}\int_0^a\int_0^b q(x,y)\sin(\alpha\, x)\sin(\beta\, y)\, dxdy = \begin{cases} q_0 \text{ for sinusoidally distributed load} \\ \dfrac{16 q_0}{mn\pi^2} \text{ for uniformly distributed load} \end{cases} \tag{32}$$

Considering that the plate is subjected to in-plane compressive loads of form: $N_x^0 = \gamma_1 N_{cr}$, $N_y^0 = \gamma_2 N_{cr}$, $N_{xy}^0 = 0$ (here γ_1 and γ_2 are non-dimensional load parameters).

Substituting Eq. (29) into Eq. (28), the following problem is obtained

$$\left(\begin{bmatrix} S_{11} & S_{12} & S_{13} & S_{14} \\ S_{12} & S_{22} & S_{23} & S_{24} \\ S_{13} & S_{23} & S_{33} & S_{34} \\ S_{14} & S_{24} & S_{34} & S_{44} \end{bmatrix} - \omega^2 \begin{bmatrix} m_{11} & 0 & m_{13} & m_{14} \\ 0 & m_{22} & m_{23} & m_{24} \\ m_{13} & m_{23} & m_{33} & m_{34} \\ m_{14} & m_{24} & m_{34} & m_{44} \end{bmatrix}\right)\begin{Bmatrix} U \\ V \\ W \\ X \end{Bmatrix} = \begin{Bmatrix} 0 \\ 0 \\ 0 \\ 0 \end{Bmatrix} \tag{33}$$

Where

$$\begin{gathered} S_{11} = -\left(A_{11}\alpha^2 + A_{66}\beta^2\right), \\ S_{12} = -\alpha\beta\left(A_{12} + A_{66}\right), \\ S_{13} = \alpha\left(B_{11}\alpha^2 + B_{12}\beta^2 + 2B_{66}\beta^2\right), \\ S_{14} = \alpha\left(k_1 B_{11}^s + k_2 B_{12}^s - \left(k_1 A' + k_2 B'\right)B_{66}^s\beta^2\right), \\ S_{22} = -\left(A_{66}\alpha^2 + A_{22}\beta^2\right), \\ S_{23} = \beta\left(B_{22}\beta^2 + B_{12}\alpha^2 + 2B_{66}\alpha^2\right), \\ S_{24} = \beta\left(k_2 B_{22}^s + k_1 B_{12}^s - \left(k_1 A' + k_2 B'\right)B_{66}^s\alpha^2\right) \\ S_{33} = -\left(D_{11}\alpha^4 + 2(D_{12} + 2D_{66})\alpha^2\beta^2 + D_{22}\beta^4\right), \\ S_{34} = -k_1\left(D_{11}^s\alpha^2 + D_{12}^s\beta^2\right) + 2(k_1 A' + k_2 B')\, D_{66}^s\alpha^2\beta^2 \\ - k_2\left(D_{22}^s\beta^2 + D_{12}^s\alpha^2\right), \\ S_{44} = -k_1\left(H_{11}^s k_1 + H_{12}^s k_2\right) - (k_1 A' + k_2 B')^2 H_{66}^s\alpha^2\beta^2 \\ - k_2\left(H_{12}^s k_1 + H_{22}^s k_2\right) - (k_1 A')^2 A_{55}^s\alpha^2 - (k_2 B')^2 A_{44}^s\beta^2 \\ k = N_{cr}\left(\gamma_1\,\alpha^2 + \gamma_2\beta^2\right) \\ m_{11} = -I_0,\quad m_{13} = \alpha\, I_1,\quad m_{14} = -J_1 k_1 A'\alpha, \\ m_{22} = -I_0,\quad m_{23} = \beta\, I_1,\quad m_{24} = -k_2 B'\,\beta\, J_1, \\ m_{33} = -I_0 - I_2(\alpha^2 + \beta^2) \\ m_{34} = J_2\left(k_1\, A'\alpha^2 + k_2\, B'\beta^2\right), \\ m_{44} = -K_2\left((k_1\, A')^2\alpha^2 + (k_2\, B')^2\beta^2\right) \end{gathered} \tag{34}$$

For the case of free vibrations we have the external energy V zero, which gives k=0 and Q_{mn}=0; the vibration frequencies are obtained by solving the system of Eq. (33) in eigenvalues.

4. Results and discussion

In this section, the free vibration analysis of simply supported FG plates by the present theory is suggested for investigation. Navier solutions for the free vibration analysis of FG plates are presented by solving the eigenvalue equations.

The FG plate is taken to be made of aluminum and alumina with the following material properties:

Ceramic (Alumina, Al2O3) Ec = 380 GPa, ν = 0.3, and ρc = 3800 kg/m^3.

Ceramic (Zirconia, ZrO2) Ec = 200 GPa, ν = 0.3, and ρc = 5700 kg/m^3.

Metal (Aluminium, Al) Em = 70 GPa, ν = 0.3, and ρm = 2702 kg/m^3.

For simplicity, the following non-dimensional natural frequency parameter is used in the numerical examples.

$$\bar{\beta} = \omega h\sqrt{\rho_m / E_m} \quad , \hat{\beta} = \omega h\sqrt{\rho_c / E_c}\ , \quad \bar{\omega} = \omega\frac{a^2}{h}\sqrt{\rho_c / E_c}$$

First, we will test the precision of this theory by comparing the results of adimensional frequencies with

Table 2 Comparison of natural frequency parameter $\hat{\beta}$ of Al/ Al2O3 square plate

a/h	mode	Theory	Porosity	p = 0.5	1	4	10
5	(1,1)	Hosseini-Hashemi *et al*. (2011b) HSDT		0.1807	0.1631	0.1378	0.1301
		Hosseini-Hashemi *et al*. (2011c) FSDT	α=0	0.1805	0.1631	0.1397	0.1324
		CPT		0.1959	0.1762	0.1524	0.1467
		Mouaici *et al*. (2016)	α=0	0.1807	0.1631	0.1397	0.1301
			α=0.1	0.1806	0.1599	0.1280	0.1195
			α=0.2	0.1803	0.1552	0.1111	0.1009
		Present	α=0	0.1807	0.1631	0.1378	0.1300
			α=0.1	0.1806	0.1599	0.1280	0.1195
			α=0.2	0.1804	0.1553	0.1110	0.1008
	(1,2)	Hosseini-Hashemi *et al*. (2011b) HSDT		0.3989	0.3607	0.2980	0.2771
		Hosseini-Hashemi *et al*. (2011c) FSDT	α=0	0.3978	0.3604	0.3049	0.2856
		CPT		0.4681	0.4198	0.3603	0.3481
		Mouaici *et al*. (2016)	α=0	0.3988	0.3606	0.2982	0.2772
			α=0.1	0.3991	0.3544	0.2776	0.2534
			α=0.2	0.3991	0.3453	0.2428	0.2128
		Present	α=0	0.3989	0.3607	0.2979	0.2771
			α=0.1	0.3991	0.3545	0.2773	0.2531
			α=0.2	0.3992	0.3454	0.2425	0.2123
	(2,2)	Hosseini-Hashemi *et al*. (2011b) HSDT		0.5803	0.5254	0.4284	0.3948
		Hosseini-Hashemi *et al*. (2011c) FSDT	α=0	0.5779	0.5245	0.4405	0.4097
		CPT		0.7184	0.6425	0.5478	0.5306
		Mouaici *et al*. (2016)	α=0	0.5801	0.5253	0.4288	0.3950
			α=0.1	0.5810	0.5171	0.4000	0.3601
			α=0.2	0.5816	0.5050	0.3517	0.3018
		Present	α=0	0.5803	0.5254	0.4284	0.3948
			α=0.1	0.5811	0.5172	0.3994	0.3597
			α=0.2	0.5817	0.5051	0.3512	0.3009
10	(1,1)	Hosseini-Hashemi *et al*. (2011b) HSDT		0.0490	0.0442	0.0381	0.0364
		Hosseini-Hashemi *et al*. (2011c) FSDT	α=0	0.0490	0.0442	0.0382	0.0366
		CPT		0.0502	0.0452	0.0392	0.0377
		Mouaici *et al*. (2016)	α=0	0.0490	0.0441	0.0380	0.0363
			α=0.1	0.0489	0.0432	0.0353	0.0336
			α=0.2	0.0489	0.0418	0.0304	0.0285
		Present	α=0	0.0490	0.0442	0.0381	0.0364
			α=0.1	0.0489	0.0432	0.0353	0.0336
			α=0.2	0.0488	0.0419	0.0304	0.0285
	(1,2)	Hosseini-Hashemi *et al*. (2011b) HSDT		0.1174	0.1059	0.0903	0.0856
		Hosseini-Hashemi *et al*. (2011c) FSDT	α=0	0.1173	0.1059	0.0911	0.0867
		CPT		0.1239	0.1115	0.0966	0.0930
		Mouaici *et al*. (2016)	α=0	0.1173	0.1059	0.0902	0.0856
			α=0.1	0.1172	0.1037	0.0837	0.0788
			α=0.2	0.1170	0.1006	0.0724	0.0668
		Present	α=0	0.1174	0.1059	0.0902	0.0856
			α=0.1	0.1173	0.1037	0.0837	0.0788
			α=0.2	0.1170	0.1006	0.0724	0.0667

Table 2 Continued

		Hosseini-Hashemi *et al*. (2011b) HSDT		0.1807	0.1631	0.1378	0.1301
		Hosseini-Hashemi *et al*. (2011c) FSDT	α=0	0.1805	0.1631	0.1397	0.1324
		CPT		0.1959	0.1762	0.1524	0.1467
			α=0	0.1807	0.1631	0.1379	0.1301
10	(2,2)	Mouaici *et al*. (2016)	α=0.1	0.1631	0.1599	0.1280	0.1195
			α=0.2	0.1599	0.1552	0.1111	0.1009
			α=0	0.1807	0.1631	0.1378	0.1300
		Present	α=0.1	0.1806	0.1599	0.1280	0.1195
			α=0.2	0.1804	0.1553	0.1110	0.1008
		Hosseini-Hashemi *et al*. (2011b) HSDT		0.0125	0.0113	0.0098	0.0094
		Hosseini-Hashemi *et al*. (2011c) FSDT	α=0	0.0125	0.0113	0.0098	0.0094
		CPT		0.0126	0.0114	0.0099	0.0095
			α=0	0.0125	0.0113	0.0098	0.0094
20	(1,1)	Mouaici *et al*. (2016)	α=0.1	0.0125	0.0110	0.0090	0.0087
			α=0.2	0.0124	0.0106	0.0078	0.0074
			α=0	0.0125	0.0113	0.0098	0.0094
		Present	α=0.1	0.0125	0.0111	0.0091	0.0087
			α=0.2	0.0125	0.0107	0.0078	0.0074

Table 3 Comparison of frequency parameter of Al/ Al_2O_3 rectangular plate (b=2a)

a/h	mode	Theory	Porosity	p				
				1	2	5	8	10
		Hosseini-Hashemi *et al*. (2011c) FSDT	α=0	2.6473	2.4017	2.2528	2.1985	2.1677
			α=0	2.6476	2.3952	2.2285	2.1707	2.1414
		Mouaici*et al*. (2016)	α=0.1	2.5934	2.2740	2.0610	2.0009	1.9723
	(1,1)		α=0.2	2.5150	2.0819	1.7655	1.6971	1.6703
			α=0	2.6475	2.3949	2.2272	2.1696	2.1407
		Present	α=0.1	2.5934	2.2737	2.0594	1.9993	1.9711
			α=0.2	2.5150	2.0817	1.7638	1.6948	1.6683
		Hosseini-Hashemi *et al*. (2011c) FSDT	α=0	4.0773	3.6953	3.4492	3.3587	3.3094
			α=0	4.0782	3.6812	3.3966	3.2987	3.2529
		Mouaici *et al*. (2016)	α=0.1	3.9982	3.4997	3.1417	3.0358	2.9893
5	(1,2)		α=0.2	3.8821	3.2118	2.6966	2.5724	2.5249
			α=0	4.07809	3.68052	3.39381	3.29642	3.25135
		Present	α=0.1	3.99813	3.49907	3.13835	3.03251	2.98685
			α=0.2	3.88199	3.21141	2.69300	2.56756	2.52060
		Hosseini-Hashemi *et al*. (2011c) FSDT	α=0	6.2626	5.6695	5.2579	5.1045	5.0253
			α=0	6.2664	5.6403	5.1481	4.9804	4.9085
		Mouaici *et al*. (2016)	α=0.1	6.1508	5.3723	4.7631	4.5748	4.4985
	(1,3)		α=0.2	5.9821	4.9466	4.1001	3.8729	4.9804
			α=0	6.2662	5.6390	5.1425	4.9758	4.9055
		Present	α=0.1	6.1507	5.3711	4.7564	4.5683	4.4937
			α=0.2	5.9820	4.9458	4.0928	3.8633	3.7798

those of the literature. In this part, various numerical examples are described, discussed and compared with other existing theories such as the theory of hyperbolic shear deformation presented by Mouaici *et al*. (2016), classical plate theory (CPT), first-order shear deformation plate theory (FSDPT) (Hosseini-Hashemi *et al.* 2011c), the exact

Table 3 Continued

5	(2,1)	Hosseini-Hashemi *et al*. (2011c) FSDT	α=0	7.7811	7.1189	6.5749	5.9062	5.7518
		Mouaici *et al*. (2016)	α=0	7.8762	7.0768	6.4153	6.1909	6.0995
			α=0.1	7.7369	6.7490	5.9372	5.6808	5.5811
			α=0.2	7.5330	6.2278	5.1208	4.8076	4.6922
		Present	α=0	7.8762	7.0751	6.4074	6.1846	6.0954
			α=0.1	7.7369	6.7474	5.9277	5.6717	5.5745
			α=0.2	7.5330	6.2268	5.1105	4.7941	4.6804
10	(1,1)	Hosseini-Hashemi *et al*. (2011c) FSDT	α=0	2.7937	2.5386	2.3998	2.3504	2.3197
		Mouaici *et al*. (2016)	α=0	2.7937	2.5365	2.3920	2.3414	2.3112
			α=0.1	2.7328	2.4031	2.2122	2.1643	2.1370
			α=0.2	2.6452	2.1921	1.8894	1.8396	1.8189
		Present	α=0	2.7937	2.5364	2.3916	2.3411	2.3110
			α=0.1	2.7329	2.4030	2.2117	2.1638	2.1366
			α=0.2	2.6453	2.1921	1.8889	1.8390	1.8182
	(1,2)	Hosseini-Hashemi *et al*. (2011c) FSDT	α=0	4.4192	4.0142	3.7881	3.7072	3.6580
		Mouaici *et al*. (2016)	α=0	4.4193	4.0092	3.7693	3.6855	3.2529
			α=0.1	4.3243	3.8001	3.4859	3.4043	2.9893
			α=0.2	4.1875	3.4693	2.9792	2.8922	2.5249
		Present	α=0	4.4192	4.0089	3.7682	3.6846	3.6368
			α=0.1	4.3243	3.7999	3.4847	3.4031	3.3592
			α=0.2	4.1874	3.4691	2.9778	2.8903	2.8548
	(1,3)	Hosseini-Hashemi*et al*. (2011c) FSDT	α=0	7.0512	6.4015	6.0247	5.8887	5.8086
		Mouaici *et al*. (2016)	α=0	7.0516	6.3893	5.9790	5.8362	5.7590
			α=0.1	6.9033	6.0604	5.5295	5.3858	5.3128
			α=0.2	6.6891	5.5398	4.7305	4.5720	4.5085
		Present	α=0	7.0515	6.3886	5.9765	5.8341	5.7575
			α=0.1	6.9032	6.0598	5.5265	5.3827	5.3105
			α=0.2	6.6890	5.5393	4.7272	4.5675	4.5045
	(2,1)	Hosseini-Hashemi *et al*. (2011c) FSDT	α=0	9.0928	8.2515	7.7505	7.5688	7.4639
		Mouaici *et al*. (2016)	α=0	9.0935	8.2319	7.6772	7.4847	7.3845
			α=0.1	8.9053	7.8123	7.1001	6.9022	6.8058
			α=0.2	8.6331	7.1479	6.0788	5.8564	5.7685
		Present	α=0	9.0933	8.2309	7.6731	7.4813	7.3821
			α=0.1	8.9051	7.8114	7.0953	6.8974	6.8021
			α=0.2	8.6329	7.1472	6.0736	5.8493	5.7621

3D solution (Vel and Batra 2004), and the theory of High order shear strain (HSDT) (Hosseini-Hashemi *et al*. 2011b, Matsunaga 2008).

Table 1 presents a comparison of the fundamental frequency $\bar{\beta}$, according to these results we see that there is a great agreement between our results and the results obtained by Mouaici *et al*. (2016), and Hosseini-Hashemi *et al*. (2011b, c), and a little big compared to the exact solution presented by Vel and Batra (2004), and a little small compared to the results of the classical theory (CPT) for the case of the perfect plate (α = 0).

In Table 2, using various plates' theories for the comparison of the natural frequency paramete$r$ $\hat{\beta}$ of a square plate Al/Al2O3 with different thickness ratios (a/h) and power law, index P. The results of the present model in the case of the perfect plate (α = 0) is in good agreement with those obtained by Hosseini-Hashemi *et al*. (2011b, c) and Mouaici *et al*. (2016). Moreover, the results of classical plate theory (CPT) overestimate the natural frequency of FGM plates, especially for thick plate at higher vibration modes. Furthermore, it can be shown that the frequencies decrease with increasing porosity (α). When the power law index P increases for the FGM plates, the natural frequency decreases. These frequencies are also sensitive to the variation of the ratio a/h.

A comparison of the frequency v of the perfect and

Table 4 First nine frequency parameter of Al/Al$_2$O$_3$ square plate (a/h=5)

Mode N°	Theory	Porosity	p					
			0.5	1	2	5	10	100
1(1,1)	Mouaici *et al.* (2016)	α=0	4.5181	4.0782	3.6812	3.3966	3.2529	2.8175
		α=0.1	4.5158	3.9982	3.4997	3.1417	2.9893	2.5267
		α=0.2	4.5096	3.8821	3.2118	2.6966	2.5249	2.0688
	Present	α=0	4.5180	4.0781	3.6805	3.3938	3.2514	2.8204
		α=0.1	4.5157	3.9981	3.4991	3.1383	2.9868	2.5273
		α=0.2	4.5095	3.8820	3.2114	2.6930	2.5206	2.0697
2(2,1)	Mouaici *et al.* (2016)	α=0	9.9714	9.0164	8.0925	7.3040	6.9318	6.1291
		α=0.1	9.9783	8.8616	7.7240	6.7612	6.3365	5.4824
		α=0.2	9.9797	8.6343	7.1378	5.8394	5.3223	4.4593
	Present	α=0	9.9715	9.0166	8.0905	7.2944	6.9270	6.1369
		α=0.1	9.9784	8.8617	7.7223	6.7496	6.3286	5.4854
		α=0.2	9.9798	8.6345	7.1367	5.8268	5.3081	4.4634
3(1,2)	Mouaici *et al.* (2016)	α=0	9.9714	9.0164	8.0925	7.3040	6.9318	6.1291
		α=0.1	9.9783	8.8616	7.7240	6.7612	6.3365	5.4824
		α=0.2	9.9797	8.6343	7.1378	5.8394	5.3223	4.4593
	Present	α=0	9.9715	9.0166	8.0905	7.2944	6.9270	6.1369
		α=0.1	9.9784	8.8617	7.7223	6.7496	6.3286	5.4854
		α=0.2	9.9798	8.6345	7.1368	5.8268	5.3081	4.4634
4(2,2)	Mouaici *et al.* (2016)	α=0	14.5049	13.1339	11.7508	10.4660	9.8768	8.8372
		α=0.1	14.5261	12.9296	11.2462	9.6970	9.0043	7.8932
		α=0.2	14.5423	12.6272	10.4411	8.4136	7.5460	6.3957
	Present	α=0	14.5064	13.1354	11.7487	10.4506	9.8703	8.8508
		α=0.1	14.5275	12.9311	11.2445	9.67822	8.9925	7.8999
		α=0.2	14.5436	12.6286	10.4406	8.39291	7.5231	6.4043
5(3,1)	Mouaici *et al.* (2016)	α=0	17.1907	15.5781	13.9180	12.3165	11.5907	10.4286
		α=0.1	17.2224	15.3488	13.3393	11.4184	10.5546	9.3081
		α=0.2	17.2502	15.0078	12.4146	9.9325	8.8382	7.5288
	Present	α=0	17.1939	15.5813	13.9166	12.2984	11.5840	10.4464
		α=0.1	17.2254	15.3518	13.3383	11.3958	10.5410	9.3179
		α=0.2	17.2529	15.0107	12.4152	9.9073	8.8108	7.5409
6(1,3)	Mouaici *et al.* (2016)	α=0	17.1907	15.5781	13.9180	12.3165	11.5907	10.4286
		α=0.1	17.2224	15.3488	13.3393	11.4184	10.5546	9.3081
		α=0.2	17.2502	15.0078	12.4146	9.9325	8.8382	7.5288
	Present	α=0	17.19387	15.58130	13.91658	12.29840	11.58401	10.44643
		α=0.1	17.22541	15.35184	13.33835	11.39582	10.54106	9.31793
		α=0.2	17.25290	15.01068	12.41521	9.90734	8.81078	7.54093
7(3,2)	Mouaici *et al.* (2016)	α=0	20.8537	18.9173	16.8757	14.8221	13.9024	12.5875
		α=0.1	20.9019	18.6582	16.2029	13.7530	12.6443	11.2264
		α=0.2	20.9481	18.2705	15.1256	12.0027	10.5816	9.0621
	Present	α=0	20.8603	18.9239	16.8765	14.8013	13.8967	12.6124
		α=0.1	20.9081	18.6645	16.2042	13.7262	12.6296	11.2416
		α=0.2	20.9538	18.2763	15.1288	11.9724	10.5488	9.0802

imperfect rectangular plate Al/Al$_2$O$_3$ for different values of the power law index P and thickness ratio (a/h) is presented in Table 3. It can be seen that there is has a great agreement between our results and the results obtained by Mouaici *et*

Table 4 Continued

8(2,3)	Mouaici *et al.* (2016)	α=0	20.8537	18.9173	16.8757	14.8221	13.9024	12.5875
		α=0.1	20.9019	18.6582	16.2029	13.7530	12.6443	11.2264
		α=0.2	20.9481	18.2705	15.1256	12.0027	10.5816	9.0621
	Present	α=0	20.8603	18.9239	16.8765	14.8013	13.8967	12.6124
		α=0.1	20.9081	18.6645	16.2042	13.7262	12.6296	11.2416
		α=0.2	20.9538	18.2763	15.1288	11.9724	10.5487	9.0802
9(4,1)	Mouaici *et al.* (2016)	α=0	25.2274	22.9124	20.4125	17.7953	16.6351	15.1525
		α=0.1	25.2978	22.6233	19.6365	16.5287	15.1139	13.5042
		α=0.2	25.3690	22.1875	18.3910	14.4786	12.6451	10.8801
	Present	α=0	25.2402	22.9251	20.4180	17.7735	16.6330	15.1878
		α=0.1	25.3100	22.6354	19.6426	16.49900	15.1002	13.5278
		α=0.2	25.3805	22.1989	18.3994	14.4439	12.6078	10.9072

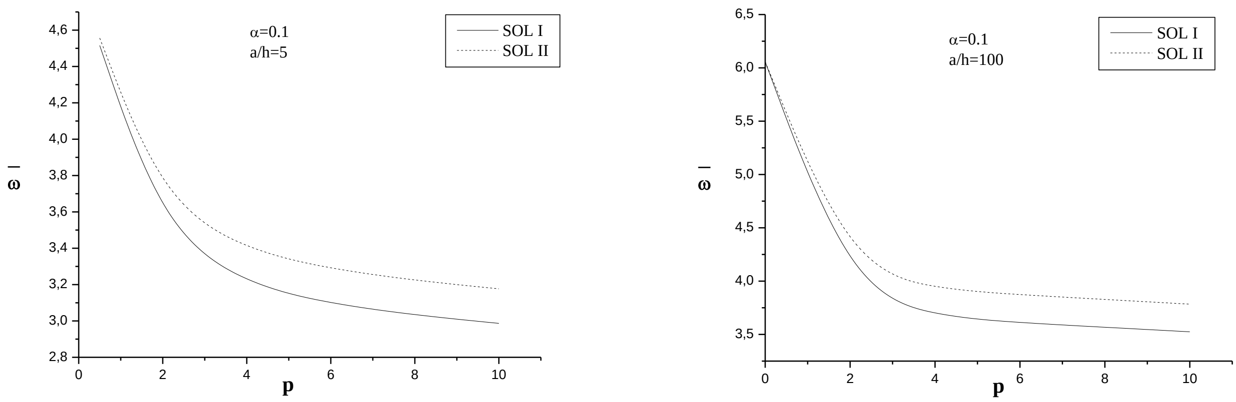

(a) (b)

Fig. 1 Influence of the power law index of the imperfect platen (α=0.1) on the frequency, (a) a/h=5 and (b) a/h=100

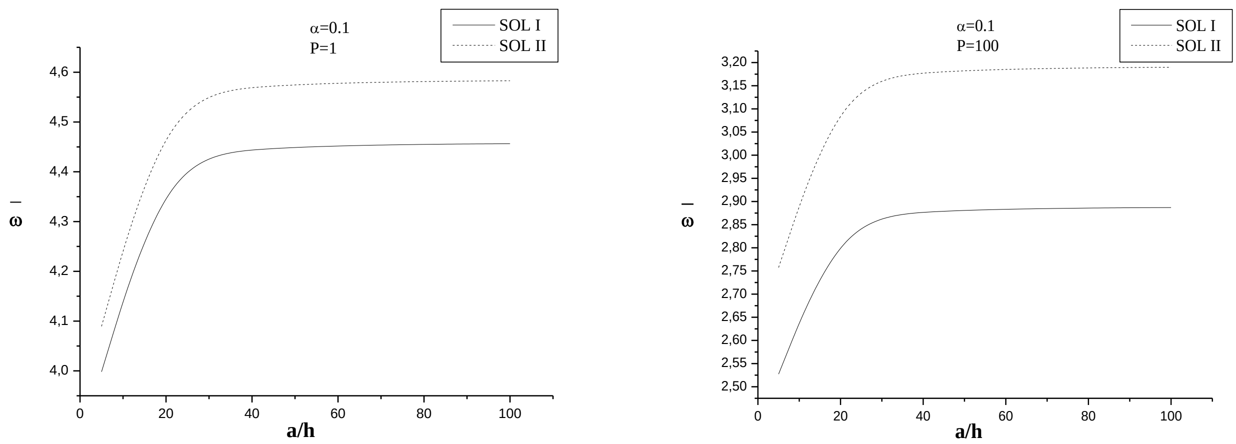

(a) (b)

Fig. 2 Influence of thickness ratio of the imperfect plate (α=0.1) on the frequency, (a) P=1 and (b) P=100

al. (2016), and a small difference with the results of Hosseini-Hashemi *et al*. (2011c); this is due to the different approaches used to predict natural frequencies. The first theory of shear deformation (FSDT) presented by Hosseini-Hashemi *et al*. (2011c) have five unknowns contrary to the present theory that use four unknowns. In addition, the frequency decreases with the existence of an imperfection in the plate (a ¹ 0).

In Table 4, another comparison with the results of Mouaici *et al*. (2016) for the first nine modes of the frequency v of a square plate Al/Al_2O_3 for different values of the power law index P and a thickness ratio (a/h = 5). Here too, the results are in great agreement with those of Mouaici *et al* (2016).

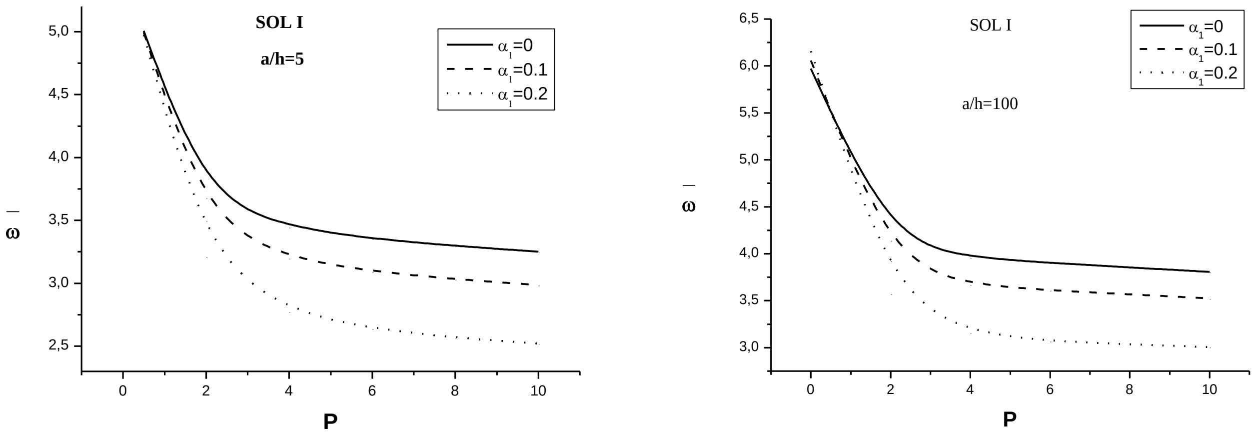

(a) (b)

Fig. 3 The effect of power law index of FG square plate on fundamental frequency parameter, (a) a/h=5 and (b) a/h=100

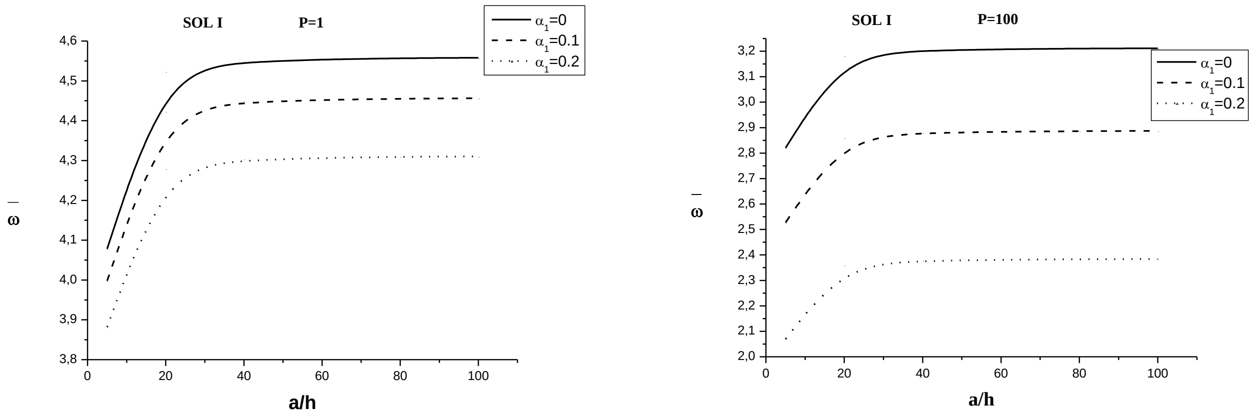

(a) (b)

Fig. 4 Variation of the adimensional frequency as a function of the thickness ratio a/h and porosity coefficient α, (a) P=1 and (b) P=100

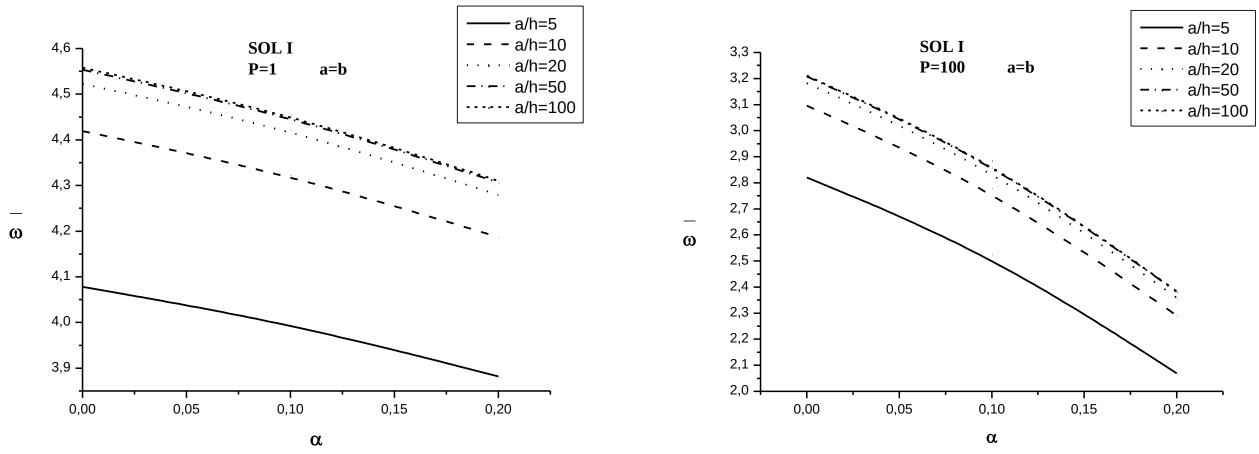

(a) (b)

Fig. 5 Variation of the adimensional frequency according to the porosity for different thickness ratio a/h, (a) P=1 and (b) P=100

In Fig. 1(a) and (b), we present a comparison between two solutions of porosity by plotting the variation of frequency. The porosity coefficient is taken α=0.1 and the thickness of the plate is h=0.2 m (Fig. 1(a)) and h=0.01 m (Fig. 1(b)). It can be seen that the frequency decrease with the increase of the power law index and the solution II provides higher frequencies than those of solution I. This is due to distributions of porosity across thickness. Indeed, the linear.

Distribution of porosity (solution II) and constant distribution (solution I) of porosity are considerably different to induce a different in results.

We study the variation of the adimensional frequency as a function of the thickness ratio a/h for the two distributions of the porosity for the power law index P = 1 and P = 100.

In Fig. 2(a) and (b). It has been found that increasing the thickness ratio increases the adimensional frequency.

Fig. 3(a) and 3(b), present the variation of the frequency parameter with power law index P is given for a/h=5 and a/h=100 respectively. According to these figures, the frequency parameter decreases with increasing index P and porosity parameter a.

Figs. 4(a) and 3(b) depict the fundamental frequency parameters versus the thickness ratio of FGM plate for p=1 and p=100 respectively. It is seen that the results increase as the thickness ratio of the plate increases for all cases (perfect and imperfect plate).

From the Fig. 5(a) and (b), the adimensional frequency is established as a function of the porosity and for different values of the thickness coefficient. It can be deduced from this curve that the increase in porosity reduces the adimensional frequency, regardless of the thickness ratio. On the contrary, an increase in the thickness ratio leads to an increase in the adimensional frequency.

5. Conclusions

A hyperbolic shear deformation theory is developed to study dynamic behaviour porous FGM plates. Unlike other shear deformation theories, only four unknown displacement functions are used in the current theory against five unknown displacement functions used in other theories. The properties of the material are assumed to vary in the direction of the thickness of the plate according to the rule of the mixture, which is reformulated to evaluate the characteristics of the material with the porosity phases. The equations of motion are derived from the Hamilton principle. Numerical validation has been done to establish the natural frequencies of FGM plates, while the emphasis is on examining the influence of several parameters. From the results obtained by the model presented, we can see that its results are very accurate compared to those obtained by Hosseini-Hashemi *et al*. (2011b, c), and Mouaici *et al*. (2016), and that the porosity contributes to significantly reducing the non-dimensional frequency. An improvement of present work will be considered in the future to consider the thickness stretching effect by using quasi-3D shear deformation models (Bessaim *et al*. 2013, Bousahla *et al*. 2014, Belabed *et al*. 2014, Fekrar *et al*. 2014, Hebali *et al*. 2014, Larbi Chaht *et al.* 2015, Hamidi *et al*. 2015, Bourada *et al*. 2015, Meradjah *et al*. 2015, Bennoun *et al*. 2016, Draiche *et al*. 2016, Sekkal *et al*. 2017b, Bouafia *et al*. 2017, Abualnour *et al*. 2018, Benchohra *et al*. 2018, Bouhadra *et al*. 2018, Ait Yahia *et al*. 2018).

References

Abdelaziz, H.H., Ait Amar Meziane, M., Bousahla, A.A., Tounsi, A., Mahmoud, S.R. and Alwabli, A.S. (2017), "An efficient hyperbolic shear deformation theory for bending, buckling and free vibration of FGM sandwich plates with various boundary conditions", *Steel Compos. Struct.*, **25**(6), 693-704.

Abualnour, M., Houari, M.S.A., Tounsi, A., Adda Bedia, E.A., Mahmoud, S.R. (2018), "A novel quasi-3D trigonometric plate theory for free vibration analysis of advanced composite plates", *Compos. Struct.*, **184**, 688-697.

Ahmed, A. (2014), "Post buckling analysis of sandwich beams with functionally graded faces using a consistent higher order theory", *Int. J. Civil Struct. Environ.*, **4**(2), 59-64.

Ahouel, M., Houari, M.S.A., Adda Bedia, E.A. and Tounsi, A. (2016) "Size-dependent mechanical behavior of functionally graded trigonometric shear deformable nanobeams including neutral surface position concept", *Steel Compos. Struct.*, **20**(5), 963-981.

Ait Amar Meziane, M., Abdelaziz, H.H., Tounsi, A. (2014), "An efficient and simple refined theory for buckling and free vibration of exponentially graded sandwich plates under various boundary conditions", *J. Sandw. Struct. Mater.*, **16**(3), 293-318.

Ait Atmane, H., Tounsi, A. and Bernard, F. (2017), "Effect of thickness stretching and porosity on mechanical response of a functionally graded beams resting on elastic foundations", *Int. J. Mech. Mater. Des.*, **13**(1), 71-84.

Ait Atmane, H., Tounsi, A., Bernard, F. and Mahmoud, S.R. (2015), "A computational shear displacement model for vibrational analysis of functionally graded beams with porosities", *Steel Compos. Struct.*, **19**(2), 369-384.

Ait Yahia, S., Ait Atmane, H., Houari, M.S.A. and Tounsi, A. (2015), "Wave propagation in functionally graded plates with porosities using various higher-order shear deformation plate theories", *Struct. Eng. Mech.*, **53**(6), 1143-1165.

Ait Yahia, S., Sekkal, M., Bousahla, A.A., Ait Atmane, H., and Tounsi, A. (2018), "A quasi-3D theory with stretching effect for buckling analysis of functionally graded sandwich plates", *Steel Compos. Struct.*, Submitted.

Akbas, S.D. (2017), "Thermal effects on the vibration of functionally graded deep beams with porosity", *Int. J. Appl. Mech.*, **9**(5), 1750076.

Al-Basyouni, K.S., Tounsi, A. and Mahmoud, S.R. (2015), "Size dependent bending and vibration analysis of functionally graded micro beams based on modified couple stress theory and neutral surface position", *Compos. Struct.*, **125**, 621-630.

Aldousari, S.M. (2017), "Bending analysis of different material distributions of functionally graded beam", *Appl. Phys. A: Mater. Sci. Proc.*, **123**(4), 296.

Attia, A., Bousahla, A.A., Tounsi, A., Mahmoud, S.R. and Alwabli, A.S. (2018), "A refined four variable plate theory for thermoelastic analysis of FGM plates resting on variable elastic foundations", *Struct. Eng. Mech.*, **65**(4), 453-464.

Attia, A., Tounsi, A., Adda Bedia, E.A. and Mahmoud, S.R. (2015), "Free vibration analysis of functionally graded plates with temperature-dependent properties using various four variable refined plate theories", *Steel Compos. Struct.*, **18**(1), 187-212.

Bakhadda, B., Bachir Bouiadjra, M., Bourada, F., Bousahla, A.A., Tounsi, A. and Mahmoud, S.R. (2018), "Dynamic and bending analysis of carbon nanotube-reinforced composite plates with elastic foundation", *Wind Struct.*, Accepted.

Belabed, Z., Bousahla, A.A., Houari, M.S.A., Tounsi, A. and Mahmoud, S.R. (2018), "A new 3-unknown hyperbolic shear deformation theory for vibration of functionally graded sandwich plate", *Earthq. Struct.*, Accepted.

Belabed, Z., Houari, M.S.A., Tounsi, A., Mahmoud, S.R. and Bég, O.A. (2014), "An efficient and simple higher order shear and normal deformation theory for functionally graded material (FGM) plates", *Compos. Part B*, **60**, 274-283.

Beldjelili, Y., Tounsi, A. and Mahmoud, S.R. (2016), "Hygro-thermo-mechanical bending of S-FGM plates resting on variable elastic foundations using a four-variable trigonometric plate theory", *Smart Struct. Syst.*, **18**(4), 755-786.

Belkorissat, I., Houari, M.S.A., Tounsi, A., Adda Bedia, E.A. and Mahmoud, S.R. (2015), "On vibration properties of functionally graded nano-plate using a new nonlocal refined four variable model", *Steel Compos. Struct.*, **18**(4), 1063-1081.

Bellifa, H., Bakora, A., Tounsi, A., Bousahla, A.A. and Mahmoud, S.R. (2017a), "An efficient and simple four variable refined plate theory for buckling analysis of functionally graded plates", *Steel Compos. Struct.*, **25**(3), 257-270.

Bellifa, H., Benrahou, K.H., Bousahla, A.A., Tounsi, A. and Mahmoud, S.R. (2017b), "A nonlocal zeroth-order shear deformation theory for nonlinear postbuckling of nanobeams", *Struct. Eng. Mech.*, **62**(6), 695-702.

Bellifa, H., Benrahou, K.H., Hadji, L., Houari, M.S.A. and Tounsi, A. (2016), "Bending and free vibration analysis of functionally graded plates using a simple shear deformation theory and the concept the neutral surface position", *J. Braz. Soc. Mech. Sci. Eng.*, **38**, 265-275.

Benadouda, M., Ait Atmane, H., Tounsi, A., Bernard, F. and Mahmoud, S.R. (2017), "An efficient shear deformation theory for wave propagation in functionally graded material beams with porosities", *Earthq. Struct.*, **13**(3), 255-265.

Benchohra, M., Driz, H., Bakora, A., Tounsi, A., Adda Bedia, E.A. and Mahmoud, S.R. (2018), "A new quasi-3D sinusoidal shear deformation theory for functionally graded plates", *Struct. Eng. Mech.*, **65**(1), 19-31.

Bennai, R., Ait Atmane, H. and Tounsi, A. (2015), "A new higher-order shear and normal deformation theory for functionally graded sandwich beams", *Steel Compos. Struct.*, **19**(3), 521-546.

Bennoun, M., Houari, M.S.A. and Tounsi, A. (2016), "A novel five variable refined plate theory for vibration analysis of functionally graded sandwich plates", *Mech. Adv. Mater. Struct.*, **23**(4), 423-431.

Bessaim, A., Houari, M.S.A., Tounsi, A., Mahmoud, S.R. and Adda Bedia, E.A. (2013), "A new higher order shear and normal deformation theory for the static and free vibration analysis of sandwich plates with functionally graded isotropic face sheets", *J. Sandw. Struct. Mater.*, **15**, 671-703.

Besseghier, A., Houari, M.S.A., Tounsi, A. and Mahmoud, S.R. (2017), "Free vibration analysis of embedded nanosize FG plates using a new nonlocal trigonometric shear deformation theory", *Smart Struct. Syst.*, **19**(6), 601-614.

Bouafia, K., Kaci, A., Houari, M.S.A., Benzair, A. and Tounsi, A. (2017), "A nonlocal quasi-3D theory for bending and free flexural vibration behaviors of functionally graded nanobeams", *Smart Struct. Syst.*, **19**(2), 115-126.

Bouderba, B., Houari, M.S.A. and Tounsi, A. (2013), "Thermomechanical bending response of FGM thick plates resting on Winkler-Pasternak elastic foundations", *Steel Compos. Struct.*, **14**(1), 85-104.

Bouderba, B., Houari, M.S.A. and Tounsi, A. and Mahmoud, S.R. (2016), "Thermal stability of functionally graded sandwich plates using a simple shear deformation theory", *Struct. Eng. Mech.*, **58**(3), 397-422.

Bouhadra, A., Tounsi, A., Bousahla, A.A., Benyoucef, S. and Mahmoud, S.R. (2018), "Improved HSDT accounting for effect of thickness stretching in advanced composite plates", *Struct. Eng. Mech.*, Accepted.

Boukhari, A., Ait Atmane, H., Houari, M.S.A., Tounsi, A., Adda Bedia, E.A. and Mahmoud, S.R. (2016), "An efficient shear deformation theory for wave propagation of functionally graded material plates", *Struct. Eng. Mech.*, **57**(5), 837-859.

Bounouara, F., Benrahou, K.H., Belkorissat, I. and Tounsi, A. (2016), "A nonlocal zeroth-order shear deformation theory for free vibration of functionally graded nanoscale plates resting on elastic foundation", *Steel Compos. Struct.*, **20**(2), 227-249.

Bourada, M., Kaci, A., Houari, M.S.A. and Tounsi, A. (2015), "A new simple shear and normal deformations theory for functionally graded beams", *Steel Compos. Struct.*, **18**(2), 409-423.

Bousahla, A.A., Benyoucef, S., Tounsi, A. and Mahmoud, S.R. (2016), "On thermal stability of plates with functionally graded coefficient of thermal expansion", *Struct. Eng. Mech.*, **60**(2), 313-335.

Bousahla, A.A., Houari, M.S.A., Tounsi, A. and Adda Bedia, E.A. (2014), "A novel higher order shear and normal deformation theory based on neutral surface position for bending analysis of advanced composite plates", *Int. J. Comput. Meth.*, **11**(6), 1350082.

Chakraverty, S. and Pradhan, K.K. (2014), "Free vibration of exponential functionally graded rectangular plates in thermal environment with general boundary conditions", *Aerosp. Sci. Technol.*, **36**, 132-156.

Chikh, A., Tounsi, A., Hebali, H. and Mahmoud, S.R. (2017), "Thermal buckling analysis of cross-ply laminated plates using a simplified HSDT", *Smart Struct. Syst.*, **19**(3), 289-297.

Draiche, K., Tounsi, A. and Mahmoud, S.R. (2016), "A refined theory with stretching effect for the flexure analysis of laminated composite plates", *Geomech. Eng.*, **11**(5), 671-690.

El-Haina, F., Bakora, A., Bousahla, A.A., Tounsi, A. and Mahmoud, S.R. (2017), "A simple analytical approach for thermal buckling of thick functionally graded sandwich plates", *Struct. Eng. Mech.*, **63**(5), 585-595.

Fahsi, A., Tounsi, A., Hebali, H., Chikh, A., Adda Bedia, E.A. and Mahmoud, S.R. (2017), "A four variable refined nth-order shear deformation theory for mechanical and thermal buckling analysis of functionally graded plates", *Geomech. Eng.*, **13**(3), 385-410.

Fekrar, A., Houari, M.S.A., Tounsi, A. and Mahmoud, S.R. (2014), "A new five-unknown refined theory based on neutral surface position for bending analysis of exponential graded plates", *Meccan.*, **49**, 795-810.

Fourn, H., Ait Atmane, H., Bourada, M., Bousahla, A.A., Tounsi, A. and Mahmoud, S.R. (2018), "A novel four variable refined plate theory for wave propagation in functionally graded material plates", *Steel Compos. Struct.*, Accepted.

Hachemi, H., Kaci, A., Houari, M.S.A., Bourada, A., Tounsi, A. and Mahmoud, S.R. (2017), "A new simple three-unknown shear deformation theory for bending analysis of FG plates resting on elastic foundations", *Steel Compos. Struct.*, **25**(6), 717-726.

Hamidi, A., Houari, M.S.A., Mahmoud, S.R. and Tounsi, A. (2015), "A sinusoidal plate theory with 5-unknowns and stretching effect for thermomechanical bending of functionally graded sandwich plates", *Steel Compos. Struct.*, **18**(1), 235-253.

Hebali, H., Tounsi, A., Houari, M.S.A., Bessaim, A. and Adda Bedia, E.A. (2014), "A new quasi-3D hyperbolic shear deformation theory for the static and free vibration analysis of functionally graded plates", *ASCE J. Eng. Mech.*, **140**, 374-383.

Hosseini-Hashemi, S., Fadaee, M. and Atashipour, S.R. (2011b), "Study on the free vibration of thick functionally graded rectangular plates according to a new exact closed-form procedure", *Compos. Struct.*

Hosseini-Hashemi, S., Fadaee, M., Rokni, D. and Taher, H. (2011a), "Exact solutions for free flexural vibration of Levy-type rectangular thick plates via third-order shear deformation plate theory", *Appl. Math. Model.*, **35**, 708-727.

Hosseini Hashemi, S.H., Rokni Damavandi Taher, H. and Omidi. M. (2008), "3-D free vibration analysis of annular plates on Pasternak elastic foundation via p-Ritz method", *J. Sound Vibr.*, **311**, 1114-1140.

Houari, M.S.A., Tounsi, A., Bessaim, A. and Mahmoud, S.R. (2016), "A new simple three-unknown sinusoidal shear deformation theory for functionally graded plates", *Steel Compos. Struct.*, **22**(2), 257-276.

Jahwari, F. and Naguib, H.E. (2016), "Analysis and homogenization of functionally graded viscoelastic porous structures with a higher order plate theory and statistical based model of cellular distribution", *Appl. Math. Model.*, **40**(3), 2190-2205.

Kaci, A., Houari, M.S.A., Bousahla, A.A., Tounsi, A. and Mahmoud, S.R. (2018), "Post-buckling analysis of shear-deformable composite beams using a novel simple two-unknown beam theory", *Struct. Eng. Mech.*, Accepted.

Kar, V.R., Mahapatra, T.R. and Panda, S.K. (2017), "Effect of different temperature load on thermal postbuckling behaviour of functionally graded shallow curved shell panels", *Compos. Struct.*, **160**, 1236-1247.

Kar, V.R. and Panda, S.K. (2013), "Free vibration responses of functionally graded spherical shell panels using finite element method", *Proceedings of the ASME 2013 Gas Turbine India Conference*.

Kar, V.R. and Panda, S.K. (2014), "Large deformation bending analysis of functionally graded spherical shell using FEM", *Struct. Eng. Mech.*, **53**(4), 661-679.

Kar, V.R. and Panda, S.K. (2015a), "Thermoelastic analysis of functionally graded doubly curved shell panels using nonlinear finite element method", *Compos. Struct.*, **129**, 202-212.

Kar, V.R. and Panda, S.K. (2015b), "Free vibration responses of temperature dependent functionally graded curved panels under thermal environment", *Lat. Am. J. Sol. Struct.*, **12**(11), 2006-2024.

Kar, V.R. and Panda, S.K. (2015c), "Large deformation bending analysis of functionally graded spherical shell using FEM", *Struct. Eng. Mech.*, **53**(4), 661-679.

Kar, V.R. and Panda, S.K. (2015d), "Nonlinear flexural vibration of shear deformable functionally graded spherical shell panel", *Steel Compos. Struct.*, **18**(3), 693-709.

Kar, V.R. and Panda, S.K. (2016a), "Post-buckling behaviour of shear deformable functionally graded curved shell panel under edge compression", *Int. J. Mech. Sci.*, **115**, 318-324.

Kar, V.R. and Panda, S.K. (2016b), "Nonlinear thermomechanical behavior of functionally graded material cylindrical/hyperbolic/elliptical shell panel with temperature-dependent and temperature-independent properties", *J. Press. Vess. Technol.*, **138**(6), 061202.

Kar, V.R. and Panda, S.K. (2016c), "Nonlinear thermomechanical deformation behaviour of P-FGM shallow spherical shell panel", *Chin. J. Aeronaut.*, **29**(1), 173-183.

Kar, V.R. and Panda, S.K. (2016d), "Geometrical nonlinear free vibration analysis of FGM spherical panel under nonlinear thermal loading with TD and TID properties", *J. Therm. Stress.*, **39**(8), 942-959.

Kar, V.R. and Panda, S.K. (2016e), "Nonlinear free vibration of functionally graded doubly curved shear deformable panels using finite element method", *J. Vibr. Contr.*, **22**(7), 1935-1949.

Kar, V.R. and Panda, S.K. (2017), "Large-amplitude vibration of functionally graded doubly-curved panels under heat conduction", *AIAA J.*, **55**(12), 4376-4386.

Kar, V.R., Panda, S.K. and Mahapatra, T.R. (2016), "Thermal buckling behaviour of shear deformable functionally graded single/doubly curved shell panel with TD and TID properties", *Adv. Mater. Res.*, **5**(4), 205-221.

Khetir, H., Bachir Bouiadjra, M., Houari, M.S.A., Tounsi, A. and Mahmoud, S.R. (2017), "A new nonlocal trigonometric shear deformation theory for thermal buckling analysis of embedded nanosize FG plates", *Struct. Eng. Mech.*, **64**(4), 391-402.

Kim, Y.W. (2005), "Temperature dependent vibration analysis of functionally graded rectangular plates", *J. Sound Vibr.*, **284**(3-5), 531-549.

Kitipornchai, S., Ke, L.L., Yang, J. and Xiang, Y. (2006), "Nonlinear vibration of edge cracked functionally graded Timoshenko beams", *J. Sound Vibr.*, **324**, 962-982.

Klouche, F., Darcherif, L., Sekkal, M., Tounsi, A. and Mahmoud, S.R. (2017), "An original single variable shear deformation theory for buckling analysis of thick isotropic plates", *Struct. Eng. Mech.*, **63**(4), 439-446.

Koizumi, M. (1997), "FGM activities in Japan", *Compos. Part B*, **28**, 1-4.

Kolahchi, R., Zarei, M.S., Hajmohammad, M.H. and Nouri, A. (2017), "Wave propagation of embedded viscoelastic FG-CNT-reinforced sandwich plates integrated with sensor and actuator based on refined zigzag theory", *Int. J. Mech. Sci.*, **130**, 534-545.

Larbi Chaht, F., Kaci, A., Houari, M.S.A., Tounsi, A., Anwar Bég, O. and Mahmoud, S.R. (2015), "Bending and buckling analyses of functionally graded material (FGM) size-dependent nanoscale beams including the thickness stretching effect", *Steel Compos. Struct.*, **18**(2), 425-442.

Mahi, A., Adda Bedia, E.A. and Tounsi, A. (2015), "A new hyperbolic shear deformation theory for bending and free vibration analysis of isotropic, functionally graded, sandwich and laminated composite plates", *Appl. Math. Model.*, **39**, 2489-2508.

Matsunaga, H. (2008), "Free vibration and stability of functionally graded plates according to a 2-D higher-order deformation theory", *Compos. Struct.*, **82**(4), 499-512.

Mehar, K., Panda, S.K., Dehengia, A., Kar, V.R. (2016), "Vibration analysis of functionally graded carbon nanotube reinforced composite plate in thermal environment", *J. Sandw. Struct. Mater.*, **18**(2), 151-173.

Mehar, K. and Panda, S.K. (2017), "Elastic bending and stress analysis of carbon nanotube-reinforced composite plate: Experimental, numerical, and simulation", *Adv. Polym. Technol.*, In Press.

Mehar, K., Panda, S.K., Bui, T.Q. and Mahapatra, T.R. (2017b), "Nonlinear thermoelastic frequency analysis of functionally graded CNT-reinforced single/doubly curved shallow shell panels by FEM", *J. Therm. Stress.*, **40**(7), 899-916.

Mehar, K., Panda, S.K. and Mahapatra, T.R. (2017a), "Theoretical and experimental investigation of vibration characteristic of carbon nanotube reinforced polymer composite structure", *J. Mech. Sci.*, **133**, 319-329.

Meksi, R., Benyoucef, S., Mahmoudi, A., Tounsi, A., Adda Bedia, E.A. and Mahmoud, S.R. (2018), "An analytical solution for bending, buckling and vibration responses of FGM sandwich plates", *J. Sandw. Struct. Mater.*, 1099636217698443.

Menasria, A., Bouhadra, A., Tounsi, A., Bousahla, A.A. and Mahmoud, S.R. (2017), "A new and simple HSDT for thermal stability analysis of FG sandwich plates", *Steel Compos. Struct.*, **25**(2), 157-175.

Meradjah, M., Kaci, A., Houari, M.S.A., Tounsi, A. and Mahmoud, S.R. (2015), "A new higher order shear and normal deformation theory for functionally graded beams", *Steel Compos. Struct.*, **18**(3), 793-809.

Mouaici, F., Benyoucef, S., Ait Atmane, H. and Tounsi, A. (2016), "Effect of porosity on vibrational characteristics of non-homogeneous plates using hyperbolic shear deformation theory", *Wind Struct*., **22**(4), 429-454.

Mouffoki, A., Adda Bedia, E.A., Houari, M.S.A., Tounsi, A. and Mahmoud, S.R. (2017), "Vibration analysis of nonlocal advanced nanobeams in hygro-thermal environment using a new two-unknown trigonometric shear deformation beam theory", *Smart Struct*. *Syst*., **20**(3), 369-383.

Park, J.S. and Kim, J.H. (2006), "Thermal postbuckling and vibration analyses of functionally graded plates", *J. Sound Vibr*., **289**(1-2), 77-93.

Pradhan, K.K. and Chakraverty, S. (2015), "Free vibration of functionally graded thin elliptic plates with various edge supports", *Struct*. *Eng*. *Mech*., **53**(2), 337-354.

Reddy, J.N. (2000), "Analysis of functionally graded plates", *Int*. *J. Numer*. *Meth*. *Eng*., **47**, 663-684.

Reddy, J.N. (2002), *Energy Principles and Variational Methods in Applied Mechanics*, Wiley, New York.

Reddy, J.N. and Cheng, Z.Q. (2001), "Three-dimensional thermomechanical deformations of functionally graded rectangular plates", *Eur*. *J*. *Mech*. *A*/*Sol*., **20**, 841-855.

Sekkal, M., Fahsi, B., Tounsi, A. and Mahmoud, S.R. (2017a), "A novel and simple higher order shear deformation theory for stability and vibration of functionally graded sandwich plate", *Steel Compos*. *Struct*., **25**(4), 389-401.

Sekkal, M., Fahsi, B., Tounsi, A. and Mahmoud, S.R. (2017b), "A new quasi-3D HSDT for buckling and vibration of FG plate", *Struct*. *Eng*. *Mech*., **64**(6), 737-749.

Shahrjerdi, A., Mustapha, F., Bayat, M. and Majid, D.L.A. (2011), "Free vibration analysis of solar functionally graded plates with temperature-dependent material properties using second order shear deformation theory", *J*. *Mech*. *Sci*. *Technol*., **25**(9), 2195-2209.

Shahsavari, D., Shahsavarib, M., Li, L. and Karami, B. (2018), "A novel quasi-3D hyperbolic theory for free vibration of FG plates with porosities resting on Winkler/Pasternak/Kerr foundation", *Aerosp*. *Sci*. *Technol*., **72**, 134-149.

Sobhy, M. (2013), "Buckling and free vibration of exponentially graded sandwich plates resting on elastic foundations under various boundary conditions", *Compos*. *Struct*., **99**, 76-87.

Taibi, F.Z., Benyoucef, S., Tounsi, A., Bachir Bouiadjra, R., Adda Bedia, E.A. and Mahmoud, S.R. (2015), "A simple shear deformation theory for thermo-mechanical behaviour of functionally graded sandwich plates on elastic foundations", *J*. *Sandw*. *Struct*. *Mater*., **17**(2), 99-129.

Tounsi, A., Houari, M.S.A., Benyoucef, S. and Adda Bedia, E.A. (2013), "A refined trigonometric shear deformation theory for thermoelastic bending of functionally graded sandwich plates", *Aerosp*. *Sci*. *Technol*., **24**(1), 209-220.

Vel, S.S. and Batra, R.C. (2004), "Three-dimensional exact solution for the vibration of functionally graded rectangular plates", *J. Sound Vibr*., **272**, 703-730.

Vo, T.P., Thai, H.T., Nguyen, T.K., Inam, F. and Lee, J. (2015a), "A quasi-3D theory for vibration and buckling of functionally graded sandwich beams", *Compos*. *Struct*., **119**, 1-12.

Vo, T.P., Thai, H.T., Nguyen, T.K., Inam, F. and Lee, J. (2015b), "Static behaviour of functionally graded sandwich beams using a quasi-3D theory", *Compos*. *Part B Eng*., **68**, 59-74.

Wattanasakulpong, N. and Ungbhakorn, V. (2014), "Linear and nonlinear vibration analysis of elastically restrained ends FGM beams with porosities", *Aerosp*. *Sci*. *Technol*., **32**(1), 111-120.

Wattanasakulpong, N., Prusty, B.G., Kelly, D.W. and Hoffman, M. (2012), "Free vibration analysis of layered functionally graded beams with experimental validation", *Mater*. *Des*., **36**, 182-190.

Woo, J., Meguid, S.A. and Ong, L.S. (2006), "Nonlinear free vibration behavior of functionally graded plates", *J. Sound Vibr*., **289**, 595-611.

Yazid, M., Heireche, H., Tounsi, A., Bousahla, A.A. and Houari, M.S.A. (2018), "A novel nonlocal refined plate theory for stability response of orthotropic single-layer graphene sheet resting on elastic medium", *Smart Struct*. Syst., **21**(1), 15-25.

Youcef, D.O., Kaci, A., Benzair, A., Bousahla, A.A. and Tounsi, A. (2018), "Dynamic analysis of nanoscale beams including surface stress effects", *Smart Struct*. *Syst*., **21**(1), 65-74.

Zemri, A., Houari, M.S.A., Bousahla, A.A. and Tounsi, A. (2015), "A mechanical response of functionally graded nanoscale beam: An assessment of a refined nonlocal shear deformation theory beam theory", *Struct*. *Eng*. *Mech*., **54**(4), 693-710

Zidi, M., Houari, M.S.A., Tounsi, A., Bessaim, A. and Mahmoud, S.R. (2017), "A novel simple two-unknown hyperbolic shear deformation theory for functionally graded beams", *Struct*. *Eng*. *Mech*., **64**(2), 145-153.

Zidi, M., Tounsi, A., Houari, M.S.A. and Bég, O.A. (2014), "Bending analysis of FGM plates under hygro-thermo-mechanical loading using a four variable refined plate theory", *Aerosp*. *Sci*. *Technol*., **34**, 24-34.

Zine, A., Tounsi, A., Draiche, K., Sekkal, M. and Mahmoud, S.R. (2018), "A novel higher-order shear deformation theory for bending and free vibration analysis of isotropic and multilayered plates and shells", *Steel Compos*. *Struct*., **26**(2), 125-137.

CC